WIND POWER MACHINES

U. Hütter

(NASA-TT-F-16195) WIND POWER MACHINES (Kanner (Leo) Associates) N75-17786
Unclas
G3/44 10250

Translation of "Windkraftmaschinen," in: Hütte, Des Ingenieurs Taschenbuch [Foundry: the Engineer's Pocketbook], Akademischen Verein Hütte, E.V. In Berlin, ed. Vol. IIA. Twenty-eight rev. ed. Wilhelm Ernst and Son (Berlin), 1954, pp. 1030-1044.

NATIONAL AERONAUTICS AND SPACE ADMINISTRATION
WASHINGTON, D. C. 20546 FEBRUARY 1975

STANDARD TITLE PAGE

1. Report No.	2. Government Accession No.	3. Recipient's Catalog No.
TT F-16,195		

4. Title and Subtitle	5. Report Date
WIND POWER MACHINES	February 1975
	6. Performing Organization Code
7. Author(s)	8. Performing Organization Report No.
U. Hütter	
	10. Work Unit No.
9. Performing Organization Name and Address	11. Contract or Grant No.
Leo Kanner Associates Redwood City, CA 94063	NASw-2481
	13. Type of Report and Period Covered
	Translation
12. Sponsoring Agency Name and Address	
National Aeronautics and Space Administration, Washington, D.C. 20546	14. Sponsoring Agency Code

15. Supplementary Notes

Translation of "Windkraftmaschinen in: Hütte, Des Ingenieurs Taschenbuch [Foundry; the Engineer's Pocketbook], Akademischen Verein Hütte, E. V. in Berlin, ed. Vol. IIA. Twenty-eight rev. ed. Wilhelm Ernst and Son (Berlin), 1954, pp. 1030-1044

16. Abstract Basic meteorological and aerodynamic features of wind power and wind wheels are discussed. The adaptation of wind power to running machinery is described. Recent (at that time) developments in wind power are illustrated, followed by a brief outline of operating properties.

PRICES SUBJECT TO CHANGE

17. Key Words (Selected by Author(s))	18. Distribution Statement
	Unclassified-Unlimited

19. Security Classif. (of this report)	20. Security Classif. (of this page)	21. No. of Pages	22. Price
Unclassified	Unclassified		

NASA-HQ

CHAPTER V. WIND POWER MACHINES

U. Hütter

A. Energy content of wind /1030*

1. Basic features. The horizontal component of the wind, which is usually the only one used, varies with time [1, 4, 17]. Short-term fluctuations over intervals of seconds or minutes are called gustiness or turbulence [16]. Wind vs. distance and time, recorded with an inertial cup anemometer, yields steadier values than gusts recordings with stagnation-pressure devices; this means that general air transport appears more uniform. The energy production of wind power plants (integrated power in kWh) exhibits a similar behavior (Fig. 1) [57].

Mean daily variation in speed over extended plane up to about 80 m elevation: rising in morning, abating in the evening. Above, reversed time variation and decreasing amplitude of fluctuation [11]. Along sea coasts and on sides of mountains, there are thermally generated land/sea or mountain/valley winds varying with the time of day ([17], p. 536); changes in meteorological conditions are superimposed on these fluctuations.

In Central Europe, there is a simple periodic variation in intensity over the year with weak winds from June to October, and strong winds from December to April [17].

Symbols

D_R	Wheel diameter [m].
E_∞	Profile lift/drag ratio [-].
E_{tot}	Total energy generated [kWh].
F_{ref} F_0	Ideal reference areas [m^2].
F_{vane}	Area of control vane [m^2].
F_R	Area of circle enclosed by wheel [m^2].

* Numbers in the margin indicate pagination in the foreign text.

H_T Height of tower (axial height of wind wheel) [m].
L Power of the facility [kW].
L_0 Ideal power content of wind [kgm/sec].
L_{inst} Rated power [kW].
M_0 Friction moment [kgm].
M_R, M_A Wheel shaft and machine moments [kgm].
R Radius (to tip of blade) [m].
R_{eff} Effective radius [m].
c_a, c_{aImp} Lift coefficients [-].
c_d Moment coefficient [-].
c_l, c_{lopt} Power coefficient [-].
c_{lid}, c_{lopt} Ideal power coefficients with zero friction [-].
c_w Axial thrust, drag coefficient [-].
$c_{w\infty}$ Profile drag coefficient [-].
f_N Frequency of power network [Hz].
h_{rel} Relative wind frequency [-].
i Gear ratio [-].
l_F Length of vane arm [m].
l_{inst} Specific power per area of circle [W/m^2].
$\dot{m}$ Mass per unit of time [kgsec/m].
n_R, n_A Rate of revolution of shaft and machine [rpm].
r Radius of a profile section [m].
t_r Width of blade at radius [m].
Δt Time interval [sec, h].
u_0 Tangential speed of wheel [m/sec].
u_e, u_3 Relative tangential speeds in wheel plane and wake [m/sec].
v_0, v_{0n}, max v_0 Wind speed in undisturbed flow [m/sec].
v_e, v_3 Velocity in wheel plane and in wake [m/sec].
v_h, v_m Most common and mean wind speeds [m/sec].
Δv Velocity change [m/sec].
w_0, w_e, w_3 Relative air speed of vane [m/sec].
z Number of blades [-].
α Angle between zero-lift direction and incident wind direction [units of arc].

β_0	Angle between plane of rotation and zero-lift direction [°].
ε	Specific annual power per area of circle [kWh/m^2/year].
η_A	Matching factor [-].
η_P	Profile friction loss factor [-].
η_R	Work factor [-].
η_Z	Blade-number loss factor [-].
θ	Blade outline function [-].
κ_G	Grid constant [-].
κ_P	Profile factor [-].
$\lambda_0 = u_0/v_0$	Wheel speed ratio [-].
λ_e	Relative speed ratio in plane of wheel [-].
ξ	Velocity reduction coefficient [-].
$\rho = \gamma/g$	Specific weight of air [kgsec^2/m]
τ	Time coordinate [-].

/1031

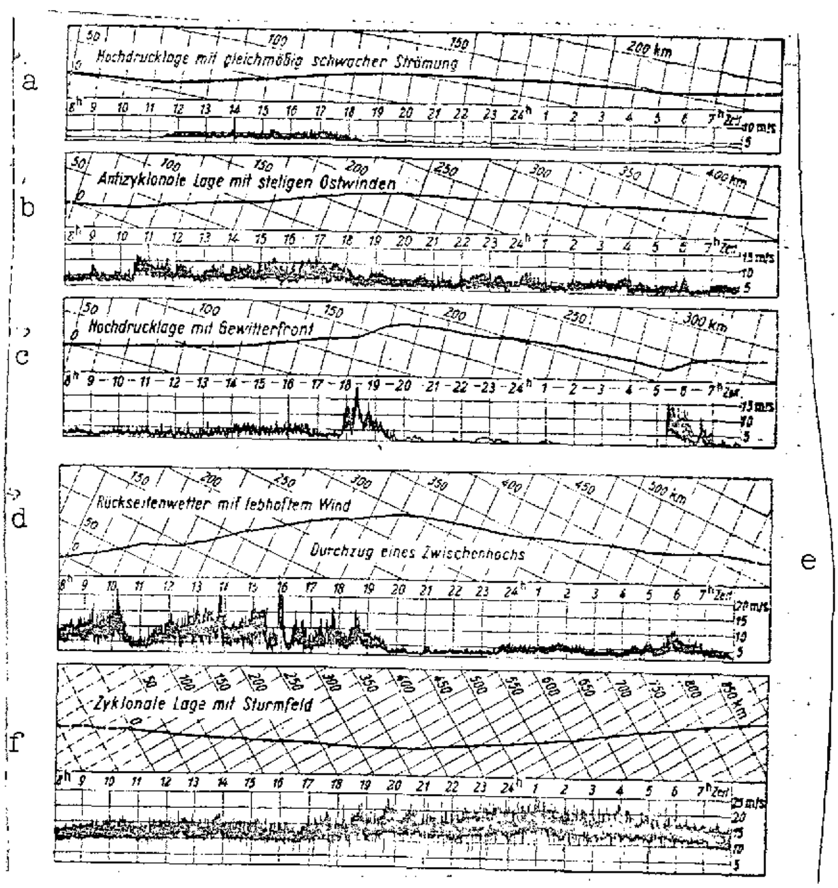

Fig. 1. Plots of wind speed and wind vs. distance for five typical weather situations (Essen-Mülheim Airport).
[Key on following page]

[Key for Fig. 1]:

a. High with uniform weak flow
b. Anticyclone with steady east wind
c. High with storm front
d. Train weather with lively wind
e. Passing through intermediate high
f. Cyclone with storm area

Zeit = time.

2. Frequency curves are the result of analyzing long-term wind observations (Fig. 2):

$$h_{rel} = \Sigma \Delta t_{\Delta v_{0n}} / \Sigma \Delta t_{\Delta v_{01}}. \tag{1}$$

$\Sigma \Delta t_{\Delta v0}$ is the sum of the time intervals Δt, over which the wind speed is within the speed intervals Δv_{01} or Δv_{0n}.

Crucial parameters: v_h the most common, and v_n the mean wind speed. In temperature zones: $v_h \approx (2/3)\, v_m$ (Wenk).

The mean wind speed v_m (hourly, daily, monthly and annual means) is known for many places and recorded (Table 1). Values for Germany are provided by the Central Office of the German Meteorological Service in Frankfurt/Main. The highest wind speeds in Central Europe are 50-65 m/sec near the ground ([32], p. 6).

TABLE 1. MEAN ANNUAL WIND SPEED IN m/sec[1] /1032

Germany	
Brocken (H)	8.7
Helgoland (C)	6.8
Hamburg	4.8
Aachen	4.6
Frankfurt/M	3.7
Buchen (Odenwald)	4.0
Goppingen	2.8
Schopfloch (H)	4.6
Friedrichshafen	3.9
Munich	3.2
Schmücke (Thur. Wald) (H)	3.7
Leipzig	3.1
Schneekoppe (H)	.0
Rest of Europe	
West Coast of Iceland (C)	7.8
Finland (coast)	6.0
Finland	3.0
Clare Morris (Irld.) (C)	4.9
Dublin Airport (C)	5.5
Shannon Airport (C)	6.0
Orkney Islands	8.0
Central England	3.2

[1] Coastal locations designated by (C), elevated locations by (H).

[TABLE 1 continued]

Brittany (C)	7.0
Normandy(C)	6.0
SE/NE France	3.2
Hela Peninsula (C)	6.3
Warsaw	3.8
Cracow	3.2
Trieste(C)	4.0
Trapani (Sicily) (C)	4.6

South Africa

Beaufort West (C)	4.4
Cape Agulhaes (C)	6.3
East London (C)	4.8
Port Elizabeth (C)	5.2
Johannesburg	3.3
Bloomfontein	3.0
Kimberley	3.2
Matroosberg	2.3

Atlantic Ocean

NE tradewind	4.9
SE tradewind	6.2

North America

Cape Cod (C)	5.7
Long Island (C)	5.4
Cape Hatteras (C)	7.2
Mississippi Valley	4.2
Miami (C)	5.3
Fort Worth (Texas)	6.2
105th meridian	3.6--4.0
Los Angeles (C)	2.8
Calgary	4.5

South America

Fernando Norbona (C)	6.9
Recife (C)	6.1
Rio de Janeiro (C)	4.3
Rio Grande del Sul (C)	5.4
São Bento	0.3
Barreiros	0.7
Caxambu Minas	0.8
Montevideo	4.6
Buenos Aires	4.4
Bahia Blanca	4.2
Commodore Riva da via	7.1
Asuncion	1.7
Rosario	3.1
Tucuman	0.9
Mendoza	1.3
Bariloche	4.6

3. <u>Relation between velocity and duration</u> as a basis for obtaining the continuous power line by integrating wind frequency curves [55]:

$$\tau = \int_{\max v_0}^{v_{0n}} h_{rel}\, dv_0 \Big/ \int_{\max v_0}^{v_0=0} h_{rel}\, dv_0 , \qquad (2)$$

8620 τ is the number of hours per year over which the wind speed is v_{0n} or greater (Fig. 3). The number of kilowatt hours per m^2 wind wheel area with total energy removal is calculated (Fig. 4) from the annual mean wind velocity. Total available energy in kWh is given by

$$E_{tot} = \varepsilon F_R \qquad (3)$$

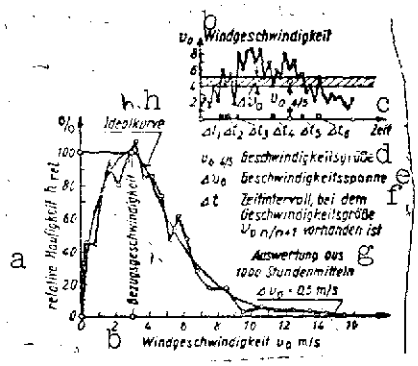

Fig. 2. Relative wind frequency, analyzed from a 45-day record (Wiesloch, Baden, April, 1946).

Key: a. Relative frequency
b. Wind speed
c. Time
d. Speed
e. Speed interval
f. Time interval in which the speed is $v_{0n/n+1}$
g. Analysis from 1,000 hourly means

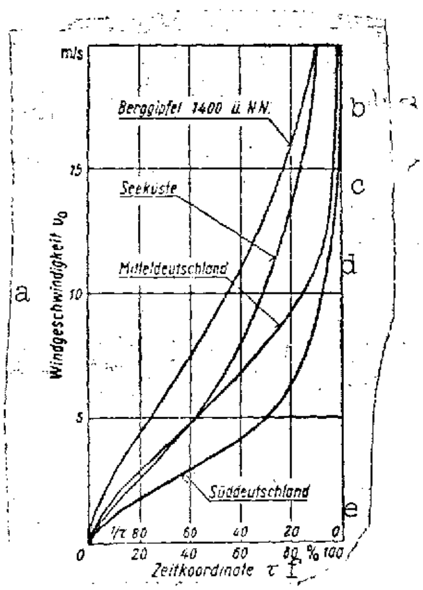

Fig. 3. Velocity profiles[1,4,17].

Key: a. Wind speed; b. Mountain top above sea level; c. sea coast; d. Central Germany; e. Southern Germany; f. Time coordinate.

With the same means and the same size facility, the specific output per unit area in W/m^2 rises in proportion to the rated power L_{inst} in kW

$$\ell_{inst} = 1000\ L_{inst}/F_R \quad (4)$$

4. All records of wind speed [4, 11, 17, 19] show a steady increase in wind speed and a general decrease in gustiness with increasing elevation above the effective surface of the Earth. A velocity maximum at the boundary of the stratosphere has been found by meteorological balloons, cirrus observations and radio-probe measurements (Fig. 5). [31].

B. Basic Aerodynamic Features

1. Basic features. Windpower machines convert the kinetic energy of air into work. The amount of air crossing the reference area F_{ref} during a unit of time (in kgsec/m)

$$\dot{m} = v_0 F_{ref} \rho$$

and this can perform work /1034 at a rate of [3, 8] (in kgm/sec)

$$L = \dot{m} v_0^2/2 = v_0^3 F_{ref} \rho/2 \qquad (5)$$

Here, v_e is the relative air speed perpendicular to the area, $\rho = \gamma/g$ is the density and γ the specific weight of air. The reference area is the projected area for rotors and the circular area swept out by the vanes for wind wheels.

The actual operating data of wind wheels is expressed in terms of the parameters of the facility by means of dimensionless coefficients:

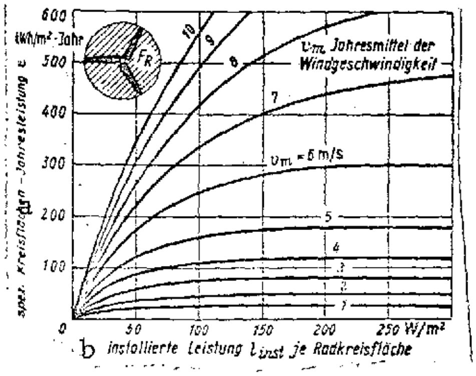

Fig. 4. Specific annual power per unit area for various annual mean wind speeds [22, 33, 56, 57]. v_m = annual mean wind speed.

Key: a. Specific annual power per unit area
b. Rated power L_{inst} per unit of wheel area
Jahr = year

Power in kW	$L = c_l F_R v_0^3 \varrho/(2 \cdot 102)$,	(6)
Torque in kgm	$M_R = c_d R F_R v_0^2 \varrho/2$,	(7)
Axial thrust in kg	$S = c_w F_R v_0^2 \varrho/2$,	(8)
Revolutions in rpm	$n = 30 \lambda_0 v_0/\pi R$.	(9)

c_l = power coefficient, c_d = moment coefficient, c_w = thrust or drag coefficient, $\lambda_0 = u_0/v_0$ wheel speed ratio (ratio between the tangential speed $u_0 = \pi Rn/30$ and the relative air speed v_0 of the wheel), R = radius to tip of blades.

2. <u>The power coefficient</u> c_l cannot be 1, even in the ideal case, since the withdrawal of energy is linked to a velocity reduction near the plane of rotation ($v_e < v_0$), and

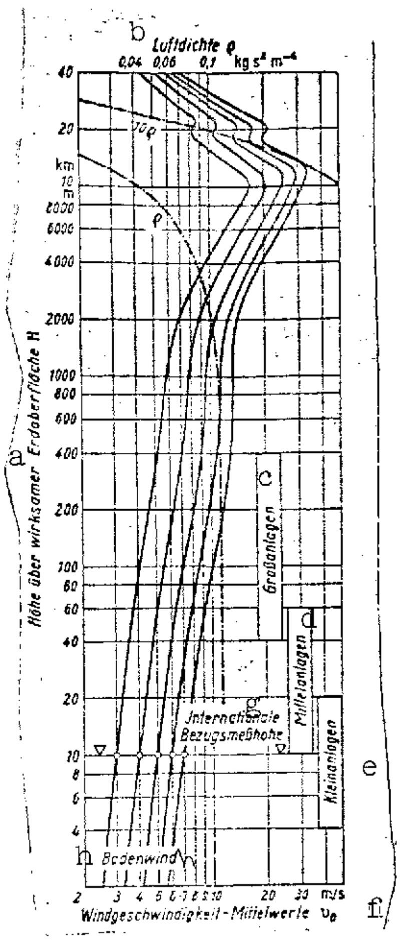

Fig. 5. Speed vs. elevation [1, 3, 4, 17, 22].

Key: a. Height above effective surface of Earth
b. Density of air
c. Large facilities
d. Medium-size facilities
e. Small facilities
f. Wind speed, mean value
g. International reference height for measurements
h. Ground wind

since the area F_0 must be less than F_R (Fig. 6) [3], because of the continuity condition

$$\Sigma v_0 F_0 = \text{const.}$$

so that the entire mass flux $\dot{m} = v_0 F_0 \rho/2$ does not cross the circular area.

The velocity reduction factor $\xi = v_3/v_0$ is crucial for the type of energy extraction.

For the wheel plane, index e), jet theory yields about half the velocity reduction and change in angular momentum in the wake of the wheel.

$$v_e = v_0/\Delta v/2, \quad u_e = u_0 + \Delta u/2.$$

Using the abbreviation

$$\sigma = \sqrt{1 + (1 - \xi)/\lambda_0^2}. \qquad (10)$$

power balance, and the laws of momentum and angular momentum conservation yield the velocities in the wheel plane (Fig. 7):

at right angles to the wheel plane

$$v_e = v_0(1+\xi)/2, \quad (11)$$

parallel to the wheel plane

$$u_e = u_0(1+\sigma)/2, \quad (12)$$

and, relative to the vane /1035
profile

$$w_e = 0{,}5\, v_0(1+\xi)\sqrt{1+\lambda_e^2}, \quad (13)$$

the effective speed ratio in the wheel plane

$$\lambda_e = \lambda_0 \frac{1+\sigma}{1+\xi}. \quad (14)$$

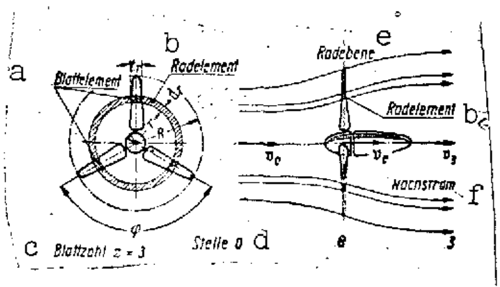

Fig. 6. Conditions near the wind wheel.

Key: a. Blade element
b. Wheel element
c. Number of blades
d. Position
e. Wheel plane
f. Weight

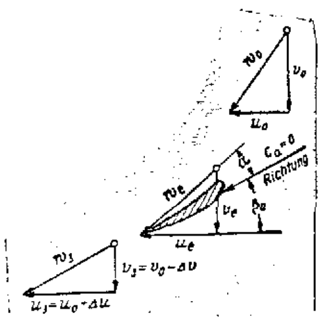

Fig. 7. Angles and velocity angles.

Key: Richtung = direction

The ideal power coefficient (Fig. 8) (ignoring the influences of profile friction, blade number and lift) with angular momentum taken into account is:

$$c_{l\,id} = \lambda_0^2(1+\xi)(\sigma-1). \quad (15)$$

The ideal optimum for $\lambda_0 \to \infty$ (zero angular momentum) and $\xi \approx 1/3$ is $c_{l\,id\,opt} = 0.5926$. Because of the substantial influence of angular momentum, a lesser reduction to $\xi \approx 1/2$ is more favorable for extremely slow wheels [22].

3. The effects of profile friction are allowed for via the loss factor

$$\eta_P = 2\lambda_0(E_\infty - \lambda_e)/[(1+\xi)(1+E_\infty\lambda_e)] \quad (16)$$

(Fig. 9) [3, 14]. $E_\infty = c_a/c_{w\infty}$ profile lift-drag ratio, c_a = lift coefficient, $c_{w\infty}$ = drag coefficient of profile, both for infinite span. Strictly speaking, $c_{l\,id}$ and η_P hold only for a wheel element at radius r and of area $dF_R = 2\pi r dr$ with an infinite number of blades.

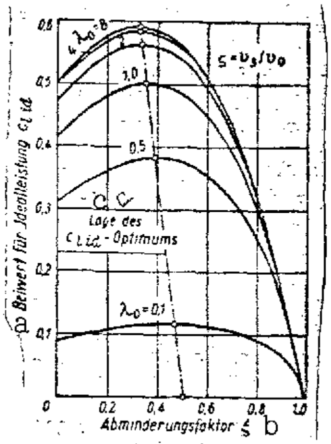

Fig. 8. Ideal power coefficient

Key: a. Coefficient for ideal power
b. Reduction factor
c. Position of $c_{l\,id}$ optimum

4. In order to ascertain the behavior of the entire wheel, values are plotted and integrated over the radius, taking deviations in ξ and c_a due to peripheral influences into account. The influence of the number of blades (Fig. 10) [18] is estimated using the blade-number loss factor.

$$\eta_z = [1 - 1{,}39/(z\sqrt{1+\lambda^2})]^2. \qquad (17)$$

z = number of blades (in Fig. 6, z = 3). For a given wheel,

$$c_l = \eta_z\,(1/R^2)\int_0^R c_{l\,id}\,d r \int_0^R \eta_p\,d r. \qquad (18)$$

the estimated effective radius is

$$R_w \approx 0{,}72\,R \qquad (19)$$

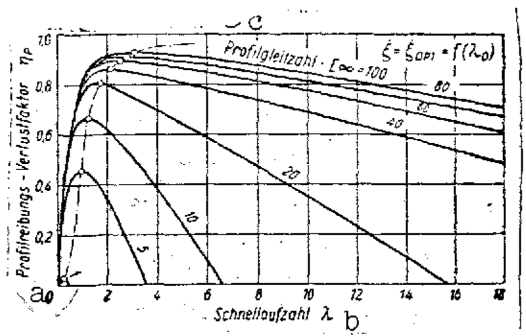

Fig. 9. Profile friction loss factor

Key: a. Profile friction loss factor
b. Speed ratio
c. Profile lift-drag ratio

This can be considered valid for the entire wheel, thus dispensing with any integrations. A condition for a possible operating state in a blade section is [22]: /1036

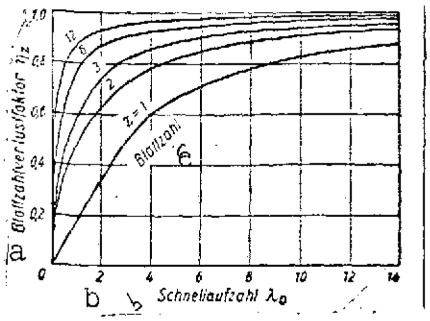

Fig. 10. Blade-number loss factor [14, 18]

Key: a. Blade-number loss factor
b. Speed ratio
c. Number of blades

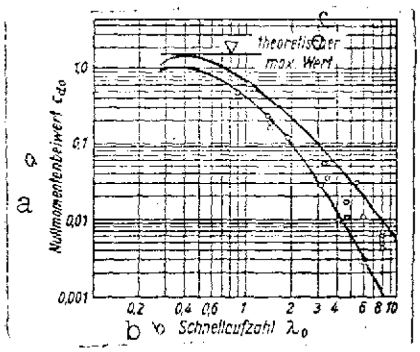

Fig. 11. Zero-moment coefficient of actual wind wheels [3,5,10,22,33].

Key: a. Zero-moment coefficient
b. Speed ratio
c. Theoretical maximum

$$c_{a\,imp} = 2\pi\kappa_P\kappa_G\alpha; \qquad (20)$$

profile factor $\kappa_P \simeq 0.92$-0.86 (profile thickness 5-18%), grid constant $\kappa_G \simeq 0.9$-1.1 (0%-7°) (Fig. 7), ([18, p. 139).

$$c_{a\,imp} = 8\pi\sqrt{2}\,\frac{r}{z\,t_r\,\lambda_0}\,\frac{\sigma\sqrt{1-1/\sigma}}{[(1+\xi)/\lambda_0]^2+(\sigma+1)^2} \qquad (21)$$

t_r = with the blade at radius r (Fig. 6).

$$\hat{\alpha} = (\cos\beta_0 - \lambda_e \sin\beta_0)/\sqrt{1+\lambda_e^2}. \qquad (22)$$

5. The moment coefficient

c_d is derived from c_1-λ_0 curves:

$$c_d = c_1/\lambda_0. \qquad (23)$$

The zero-moment coefficient c_{d0} with the wheel stopped is a function of the design speed ratio, angular variations, blade profile and outline configuration (Fig. 11). Since the blades of high-speed wheels are almost parallel to the plane of rotation, flow separates along almost the entire blade when the wheel is stationary. Therefore, moment coefficients for when these wheels are stationary are very small. The start-up properties of high-speed wheels can be improved by altering

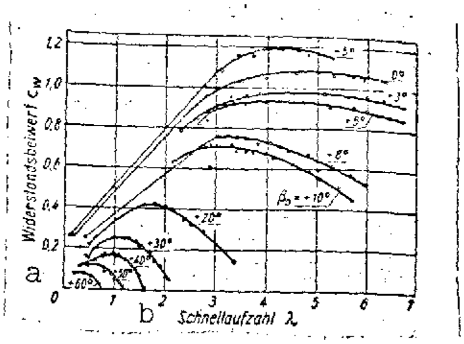

Fig. 12. Wind-tunnel measurements to determine axial thrust coefficients of a four-vane model wheel [20,22].

Key: a. Drag coeffient c_W
b. Speed ratio

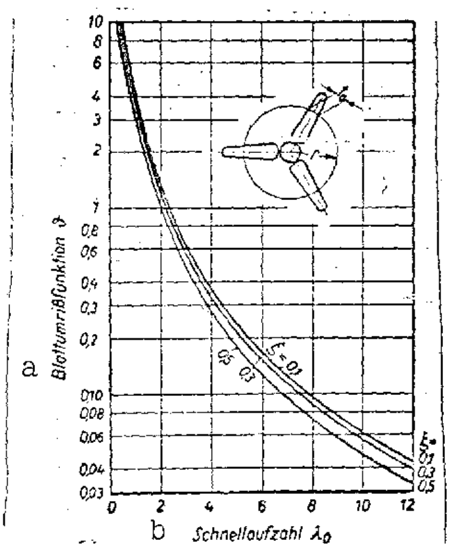

Fig. 13. Blade-outline function [22].

Key: a. Blade-outline function
b. Speed ratio

the blade orientation (automatically or manually), so that the flow adheres to the profile along most of the blade radius.

6. Drag coefficients are estimated from

$$c_w = (1 - \xi^2)(1 + \lambda_r/E_\infty). \qquad (24)$$

The profile lift coefficients c_a must be known in order to determine E_∞. Because the profile lift-drag ratio $E_\infty \to 0$ as $c_a \to 0$, c_W is relatively large for high-speed wheels even when idling. Fig. 12 shows some measurements.

7. The blade width of /1037 wind wheel vanes is obtained from the basic outline

$$t_r = r\,\vartheta / z\,c_a \qquad (25)$$

by means of the outline /1038 function

$$\vartheta = 4\pi\sqrt{2}\,\frac{\sigma - 1}{\sqrt{1 + \sigma + (1 + \xi)/\lambda_0^2}}. \qquad (26)$$

In the range of normal values, the influence of the reduction factor ξ on the outline is slight (Fig. 13). The shape obtained from Eq. (26) corresponds to the rectangular outline of airfoils and ought to be slightly corrected to give it an elliptical outline, to allow for a steady lift distribution.

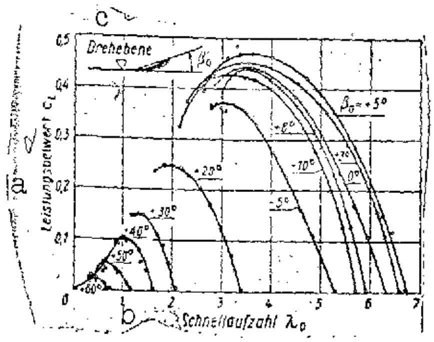

Fig. 14. Wind-tunnel measurement of power coefficients of a four-vane wind wheel [22]

Key: a. Power coefficient
b. Speed ratio
c. Plane of rotation

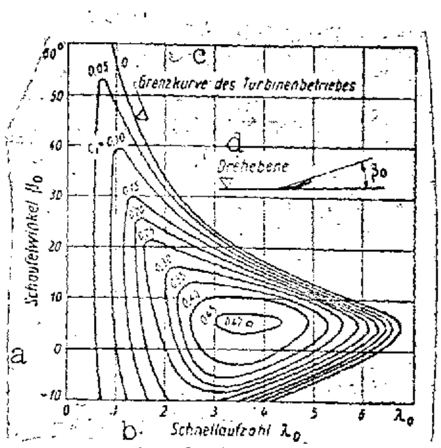

Fig. 15. Power coefficient field based on wind-tunnel measurements [22].

Key: a. Blade angle
b. Speed ratio
c. Limiting curve of turbine operation
d. Plane of rotation

8. Wind-tunnel measurements on wind wheels with different blade angles (Figs. 12, 14, and 15) show that limiting power by modifying the orientation of the blades is very effective, and also that the optimum c_l curve is an envelope for all other curves over a very wide range of speed ratios, (Fig. 15).

Comparing the c_l and c_d curves of wheels of different designs shows the superiority of the low speed wheel in starting, and that of the high-speed wheel in power and revolutions [3, 10, 20, 33, 52]. Rotors based on the cup-anemometer or the Savonius principle [51] are greatly inferior, because of the greater construction effort for a given circular area and because of lower revolutions for the same diameter and a substantially poorer power coefficient (Fig. 16) [33].

C. Adaptation to machinery

1. In order to have wind power plants and machinery or generators cooperate, stable conditions must prevail regardless of the values of v_0 and n_R;

i.e.

$$M_R(v_0, n_R) - M_0 = i M_A(n_A), \quad (27)$$

$$\mathrm{d}M_R/\mathrm{d}n_R \leq i^2 \,\mathrm{d}M_A/\mathrm{d}n_A. \quad (28)$$

M_R is the driving moment of the wind wheel, M_A is the torque of the machine being driven, M_0 is the frictional moment of the entire facility, relative to the shaft of the wind wheel and i is the gear ratio of the gearing between the wind wheel and the machine [53].

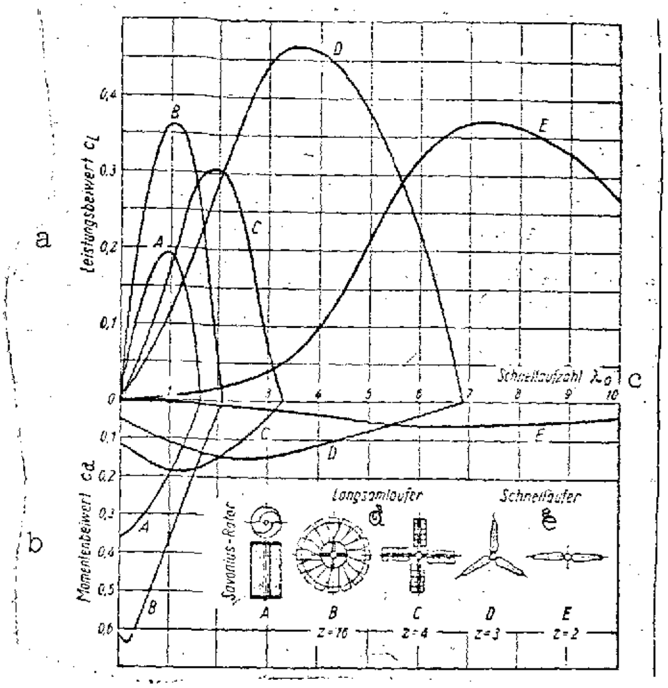

Fig. 16. Power and moment coefficients of wind wheels with different designs and speed ratios (according to Fateyev) [10,22,33, 51].

Key: a. Power coefficient
b. Moment coefficient
c. Speed ratio
d. Low-speed wheel
e. High-speed wheel

2. The efficiency

$$\eta_R = c_l(v_0, n_R)/c_{l\,\mathrm{opt}} \quad (29)$$

gives the utility of the chosen /1039 operating point of the wheel, relative to the optimum power [55]. At different wheel revolutions and wind speeds the value of η_R depends on the position of the torque-revolutions curve of the machine in the torque-revolutions field of the wind wheel (Fig. 17). Optimum compatability with good start-up behavior is obtained with d.c. double-wound generators in connection with a battery and an ohmic resistance. Mains-powered asynchronous and synchronous generators do not match as well [26, 55].

Precise study on the optimum position of the fixed number of revolutions of the wheel as determined by the mains frequency f_N and the gear ratio i in the light of power curves allowing

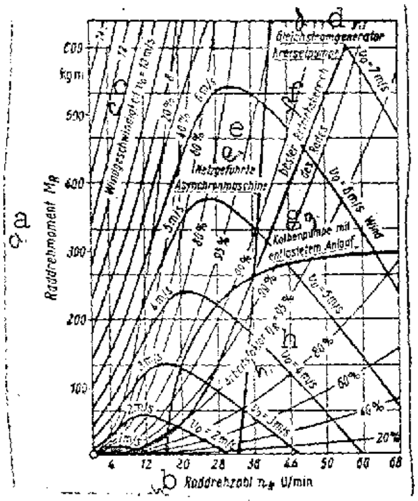

Fig. 17. Moment/revolutions/wind speed field of a facility with a wheel 20 m in diameter along with operating characteristics of generators and pumps [55].

Key:
- a. Wheel torque
- b. Wheel revolutions in rpm
- c. Wind speed
- d. A.C. generator, rotary pump
- e. Mains-driven synchronous motor run on power network
- f. Optimum operating range of wheel
- g. Reciprocating pump with reduced-load starting
- h. Efficiency

for the various values of η_R: power delivered by the facility as a function of the time coordinate τ in Fig. 18.

3. The matching coefficient compares the actual total energy delivery with the ideal output at $\eta_R = 1$ (Fig. 18).

$$\eta_A = \int_0^1 \eta_R L \, d\tau \Big/ \int_0^1 L \, d\tau. \qquad (30)$$

Matching factors of more than 90% are possible even with fixed rates of revolution [55]. When high-speed wheels are being used to drive machinery with moments independent of the rate of revolution (reciprocating pumps, wood saws, roughing mills, tool machines, etc.), couplings which are controlled by the rate of revolution or variable gear ratios must be employed in order to start with zero load [32].

D. Examples of windpower machines

1. <u>Low-speed wheel</u> (Fig. 19) with design speed ratio 1-2, 3-6 m in diameter. One-stage step-down gearing 1:2.5 to 1:3.5; crank gearing with sliding guide of lifting mechanism in tower head (Fig. 20); on square angle-bracket towers; has worked well as a machine to drive simple reciprocating pumps [5, 21, 33]. Four-vaned wheel with blades

of galvanized, curved 1-1.5 mm sheet metal turns in the lee of the tower.

Wheel disc rough-turned by weather vane. Length of vane arm $l_F \approx (2/3)\ D_R$, vane area $F_{vane} \approx F_R/8$, tower height $H_T \approx 3\text{-}5\ D_R$; controlled by turning the wheel disc, mounted off-center relative to the vertical axis of the tower, with stagnation pressure at high wind speeds against the tension of a long spring, the vane remaining in the wind direction (Fig. 21). Adjustment with chains or wire, likewise by turning the wheel disc.

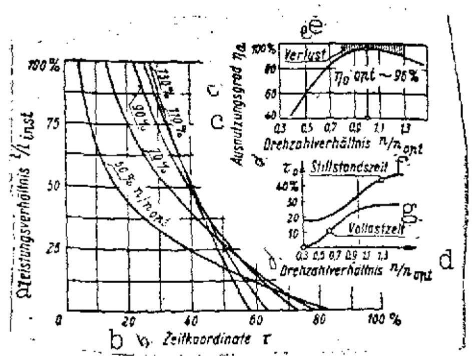

Fig. 18. Power curves for a wind power plant working together with a mains driven synchronous generator for various fixed rates of revolution [55].

Key:
- a. Power ratio
- b. Time coordinate
- c. Efficiency
- d. Ratio of rates of revolution
- e. Loss
- f. Period of stoppage
- g. Period of full load

2. Modern high-speed wheels (design speed ratio 3-9) are usually constructed as electrical facilities because of the lesser adaptation problems (Figs. 22 and 23). Guyed or free-standing very stiff tube or grid masts. Free-standing towers spread out near the base. Concrete foundations with cast steel reinforcement [11, 25, 26]. Usually constructed by hoisting up mast anchored at its base at one point [33]. In addition to the usual loads on tall structures, the towers must bear stresses due to inertial forces and moments [e.g. gyroscopic moments of the wheels). The lower edge of the wind wheel should be at least 3 m above the vortex trail of obstacles (stretchers or rows of trees). Towers of medium-size facilities (3-100 kW) are 1-3 D_R high.

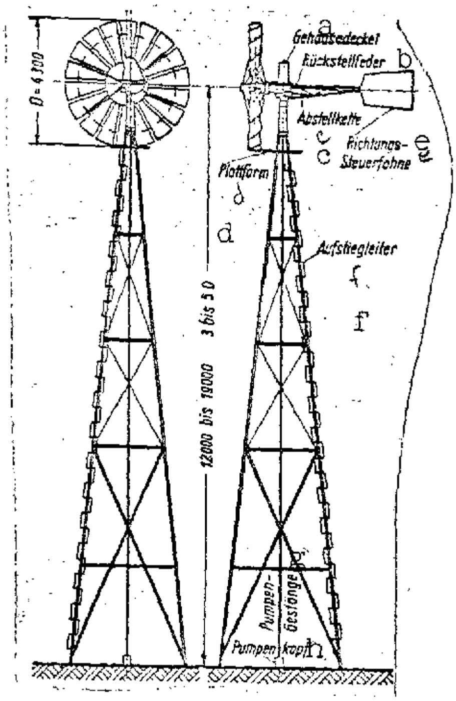

Fig. 19. Wind-power pumping plant with low-speed wheel [5, 10, 21].

Key: a. Housing cover
b. Return spring
c. Regulating chain
d. Platform
e. Direction control vane
f. Ladder
g. Pump linkage
h. Pump head
bis = to

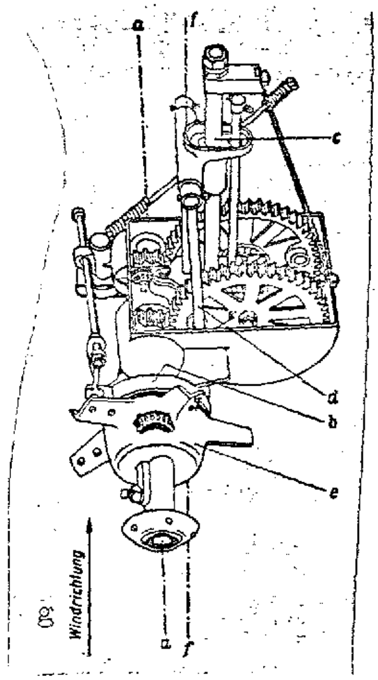

Fig. 20. Pump head gearing

aa -- Axis of wind wheel, b -- Shoe brake, locks the wheel when fully swung out, c -- Guide, d -- Connecting rod, e -- Hub of wheel, ff -- Vertical axis of tower.

Key: g. Wind direction

The vanes for wind wheels up to 5 m in diameter are made of laminated solid wood glued with synthetic resins. Larger vanes are made of light metal or sheet steel in the scooped configuration, usually with a central bar and ribs to support the skin, and /1041
rigidly attached by a flange to a welded or cast steel hub (Fig. 24) [31, 33], or mounted by several single-row or one multi-row roller bearings so that it pivots about the long axis of the

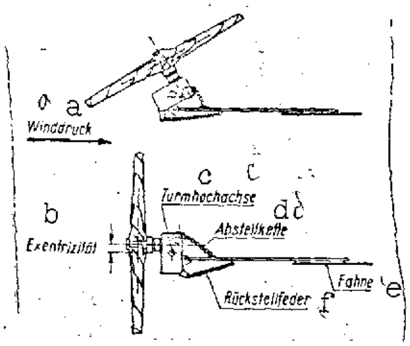

Fig. 21. Eccentric governor (eclipse control) for low-speed wheels [33].

Key: a. Wind pressure
b. Eccentricity
c. Vertical axis of tower
d. Adjusting chain
e. Vane
f. Return spring

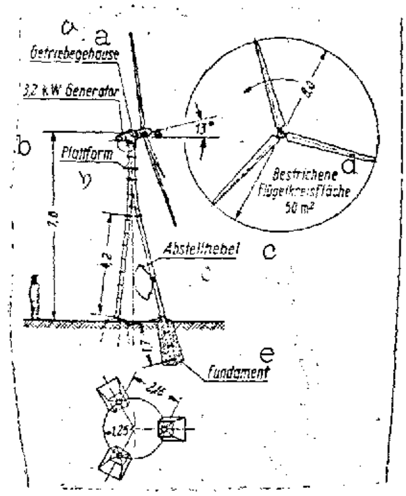

Fig. 22. Electrical wind power plant with high-speed wheel (Allgaier, Uhingen). Rated power 3.2 kW, full load reached at 6.2 m/sec wind speed.

Key: a. Gear housing
b. Platform
c. Adjusting lever
d. Circular area swept out
e. Foundation

vane (Fig. 22). The vane is pivoted by push rods or gears.

4. Tower head. In electrical facilities with attached generator [31], one- to three-stage spur-gear system, usually with ground helical gear wheels; sump lubrication preferred because of freedom from maintenance. Vibration-proof screw connections and satisfactory seals are very important [24].

Direct mechanical [26] or hydraulic servocontrol [31] of rate of revolution and torque is achieved by adjusting the blade angle. This is accomplished by a sturdy centrifugal governor. This also permits power control as pure loss regulation using the

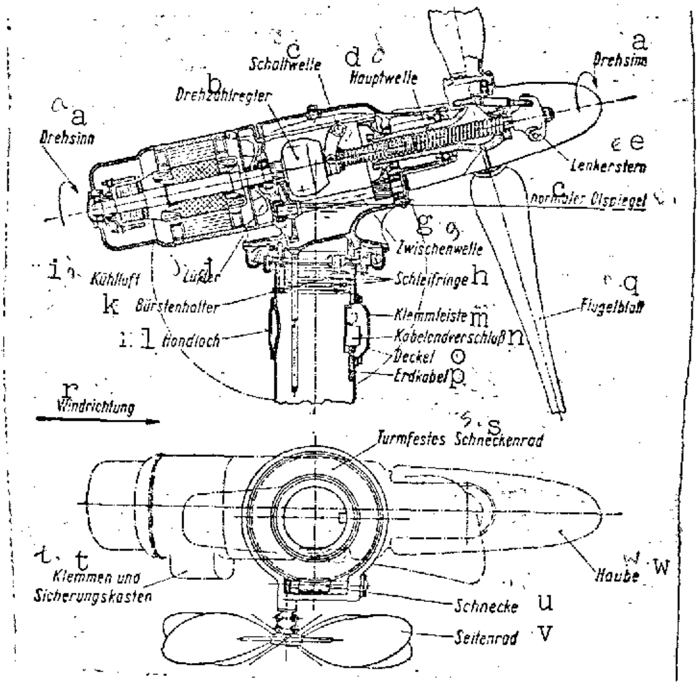

Fig. 23. Head gearing of an electrical wind power plant (Allgaier, Uhingen).

Key:

a. Direction of rotation
b. Revolutions governor
c. Gear-shift shaft
d. Main shaft
e. Guide star
f. Normal oil level
g. Intermediate shaft
h. Slip rings
i. Cool air
j. Ventilator
k. Brush holder
l. Access hole
m. Connecting block
n. Cable terminal
o. Cover
p. Ground cable
q. Blade
r. Wind direction
s. Worm gear fixed to tower
t. Terminals and fusebox
u. Worm
v. Side wheel
w. Hood

criteria of structural strength, specified range of rate of revolution, and permissible power drain (Fig. 15). With hydraulic servocontrol, additional control pulses are possible to secure against storms with wind speeds over 22 m/sec (the frequency of which is less than 0.1% of the overall time even in areas with high winds [1, 4, 17]), and to facilitate starting when the wheel is stopped by adjusting the blades. Adjustment is through linkages at the foot of the tower. The head is mounted on ball or roller bearings of large diameter or on thrust or pivot bearings [11, 33]. Directional control via self-locking worm gear [31] through side wheel (Nordwind G.m.b.H., Allgaier) or by small directional vane controlling the sense of rotation of an electric motor (Ventimotor G.m.b.H). Current drawn through copper slip rings at top of tower. The slip rings /1042 are designed like those for lifting machines.

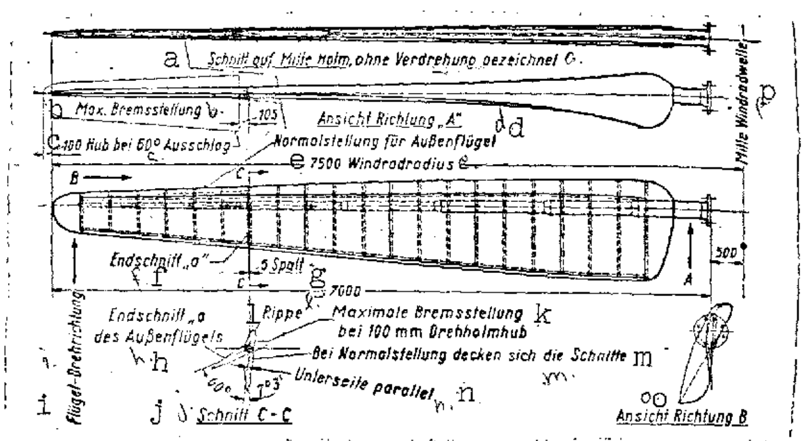

Fig. 24. Construction of a metal vane attached rigidly to hub, and control by adjustment of outer vane (Nordwind G.m.b.H).

Key:
a. Section at center of bar, drawn without twist
b. Max. braking position
c. Stroke at 60° deflection
d. View, direction A Normal position for outer vane
e. Radius of wind wheel
f. End section
g. Crack
h. End section A of outer vane
i. Direction of vane rotation
j. Section
k. Max. braking position with 100 mm rotation bar stroke
l. Rib
m. The sections coincide in normal position

[Key continued on next page]

[Key to Fig. 24 continued]

n. Underside parallel
o. View, direction B
p. Center of wind-wheel shaft

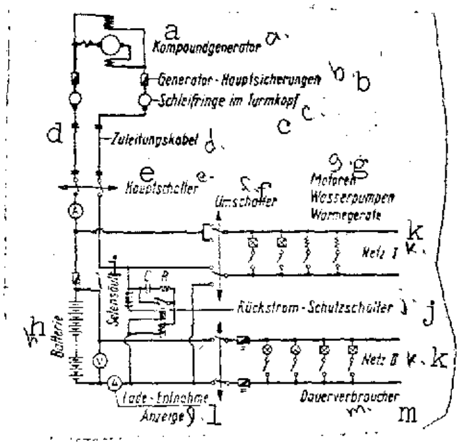

Fig. 25. Overall circuit diagram of an electrical wind power plant with compound D.C. shunt-wound generator

Key:

a. Compound generator
b. Principal generator fuses
c. Slip rings at top of tower
d. Feed cable
e. Main switch
f. Change-over switch
g. Motors, water pumps, heating units
h. Battery
i. Selenium column
j. Reverse current circuit breaker
k. Mains
l. Load display
m. Steady loads

5. Trickle chargers [21], usually a two-bladed wheel 3-4 m in diameter, generate weak currents for lighting and radios. Like lighting equipment for motor vehicles, the generators are usually equipped with Tyrill field governors and vehicle batteries. Small units generally have no gearing. They are regulated by centrifugally controlled drag surfaces or by turning toward the vane against the spring tension.

E. Operating properties of wind power machines. /1043

Wind power plants do not operate 16-35% of the time. Full load is reached only 8-28% of the time, depending on wind frequency and specific load per unit area of circle. Partial-load operation over 2/3 of total operating time, with widely fluctuating power and rate of revolution (Fig. 18) [2,7 22, 55, 57]. Therefore there must be power compensation by

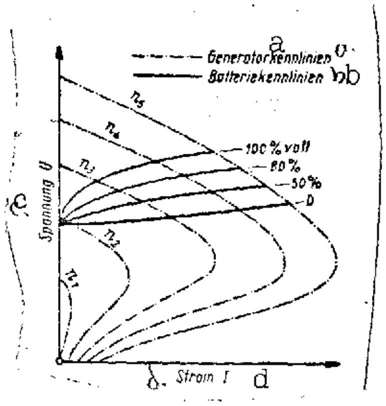

Fig. 26. Cooperation of a compound shunt-wound generator with a lead battery as buffer.

Key: a. Generator characteristics
b. Battery characteristics
c. Voltage
d. Current
voll = full

1. Appropriately designed energy storage: lead or alkaline batteries, heat storage (hot water, steam, solid), flywheel systems (Örlikon).

2. Adapting power consumption to power generation. This is possible in the manufacture of stored and mass-production goods, electrolysis, fruit drying, chopping, grinding, conveying, water pumping, etc. [56].

3. Supplying energy to powerful networks with large constant basic loads [30, 53, 55].

The simplest operating method for electrical facilities is to supply power through two separate networks, one for small loads (lighting, radio, small equipment) to a discriminating circuit breaker and a buffer battery, and the other for large loads for heating and power, fed directly from the generator without buffering (Fig. 25). The battery is charged through a double shunt-wound generator with an adjustable voltage limit (Fig. 26), in order to avoid overcharging the battery.

REFERENCES

Books

1. Assman, Die Winde in Deutschland [Winds in Germany], Braunschweig 1910, Vieweg.

2. Sabinin, Die Problème der Ausnutzung der Windenergie [Problems in exploiting wind power], Moscow, 1923.

3. Betz, Windenergie and ihre Ausnutzung durch Windmühlen. [Wind energy and its exploitation through windmills], Vandenhoek and Ruprecht, Göttingen, 1926.

4. Georgii, Flügmeteorologie [Aerometeorology], Akadem. Verlagsges, Leipzig, 1927.

5. Bilau, Die Windkraft in Theorie und Praxis [Wind power in theory and practice, Parey, Berlin, 1927.

6. Bilau, Windmühlenbau einst und jetzt [Windmill construction then and now],Schäfer, Leipzig, 1927.

7. Sabinin, Die Charakteristik einer Windkraftanlage in Abhängigkeit von Windeigenschaften [Characteristics of a wind power plant in relation to wind properties, Moscow, 1926.

8. Sabinin, Theorie einer idealen Windkraftanlage [Theory of an ideal wind power plant], Moscow, 1927.

9. Darrieus, Théorie élementaire du moulin au vent [Basic windmill theory], and Champly, Les Moteurs à vent [Wind Motors] Dumond, Paris, 1933.

10. Prandtl and Betz, Ergebnisse der Aerodynamischen Versuchsanstalt Göttingen, München und Berlin [Results of the Aerodynamic Experimental Laboratory in Göttingen, Münich, and Berlin]in 1932 through 1935, Oldenbourg.

11. Honnef, Windkraftwerke [Wind power plants],Braunschweig, 1932, Vieweg.

12. Szowheniw, Silniki Wietrzne [Wind motors], Sklad Plowny W. Ksiegarnie Technicznej, Warsaw, 1932.

13. Sektorov, Bericht über die Arbeitscharakteristiken der ersten 100 kW windelektrischen Anlage bei Balaklava [Report on operating characteristics of the first 100 kW electrical wind plant at Balaklava], Moscow, 1933.

14. Glauert, Airscrew Theory, Vol. IV, Section of Aerodynamic Theory, Springer, 1935.

15. Hipt, Windmühlenpraxis [Windmill practice], Parey, Berlin, 1937.

16. Lettau, Atmosphärische Turbulenz [Atmospheric turbulence] Akadem. Verlagsges, Leipzig, 1938.

17. Hann-Süring, Lehrbuch der Meteorologie [Text on Meteorology], Keller, Leipzig, 1939, pp. 481-678, Air motions.

18. Weinig, Die Aerodynamik der Luftschraube [Aerodynamics of the air screw], Springer, Berlin 1940.

19. Wilcox, Computations of variations of velocity with height, Vol. 3, Handbook of Aerology, 1941.

20. Hütter, The development of high-power wind wheels. Report No. 4 of the Ventimotor G.m.b.H., Weimar, 1941.

21. Schieber, Energiequelle Windkraft [Wind power as an energy source], Fackelträger, Berlin, 1942.

22. Hütter, Beitrag zur Schaffung von Gestaltungsgrundlagen für Windkraftwerke [Contribution to the basic design features of wind power plants], Dissertation, Weimar, 1942.

23. Stein, Windkraftanlagen in Dänemark [Wind power plants in Denmark], RAG Windkraft, Berlin 1942, Report 4.

24. Wilcox, Report on yawing and pitching moments of the Smith Putnam wind turbine, USA, April 1943.

25. Kleinhentz, Gewichts und Kostenvergleich von Grosswindkraftwer werken verschiedener Höhe bei gleichem Windraddurchmesser [Weight and cost comparisons of large wind power plants of different heights with the same wind wheel diamters], RAG Windkraft, Report No. 6, Berlin, 1913.

26. Konig, Der Windstromautomat 5 bis 7.5 in Bornim-Potsdam [The 5-7.5 kW wind power plant in Bornim-Potsdam] RAG Windkraft, Report No. 6, Berlin, 1943.

27. Voaden, Field Test Report No. 1 to 10 of the Smith Putnam wind turbine, USA, 1941-1943.

28. Fateyev, Wie kann die Leistungsfähigkeit der bereits vorhandenen Windmühlen gesteigert werden? [How can the output of already existing windmills be increased], Moscow, 1943.

29. Vershinin, Anleitung für den Betrieb windelektrischer Aggregate mit niedriger Leistung in der Landwirtschaft [Directive for the operation of low-power agricultural machinery driven by electricity from wind power], Moscow, 1946.

30. Sektorov, Energetische Charakteristiken der WES mit Asynchron-Generator in Zusammenarbeit mit dem öffentlichen Netz. [Energy characteristics of the WES with asynchronous generator in cooperation with the public power system] Moscow, 1947.

31. Putnam, Power from the wind, D. von Nostrand Co., Inc., New York, 1947.

32. Van Heys, Wind- and Windkraftanlagen [Wind and wind power plants, Siemens, Berlin, 1947.

33. Fateyev, Windkraftanlagen and Grosswindkraftwerke [Wind power plants and large wind power plants], Moscow, 1948.

34. Löbel, Windkraft. Grossraum-Verbundwirtschaft [Wind power. Large-area compound economy], West-Verl., Essen, 1948.

35. Andreau, L'Eoliènne nouvelle formule n'a ni Mecánisme ni Engregage [A new type of wind generator with no gears or mechanical parts], Manotention Mécanique, Paris. 1950.

36. Witte, Windkraftwerke [Wind power plants], Lang, Pössnek, 1950.

Journals

40. Elektrizitätswirtschaft, Verlagsges. der Elektrizitätswerke, Frankfurt/Main.

41. Der Elektrotechniker, VDE-Verl., Wuppertal-Elberfeld.

42. Elektrotechnische Zeitschrift (ETZ) VDE-Verl., Frankfurt/Main.

43. Archiv für Energiewirtschaft, Seifert, Berlin-Schöneberg.

44. Mechanical Engineering, Amer.Soc. Mech. Engrs., Easton, Pa.

45. Schweizer, Bauztg. Zürich, Jegher and Östertag.

46. Technik, Verl. Technik., Berlin.

47. Technik für Bauern und Gärtner, Wesel, Baden-Baden.

48. Zeitschrift für angewandte Mathematik und Mechanik (ZAMM), Akademie-Verlag., Berlin.

49. Zeitschrift für Elektrotechnik (ZfE), Enke, Stüttgart.

Important Articles

50. Pfleiderer, "Application of elementary turbine theory to calculations for wind wheels" [48], p 180 (1921).

51. Savonius, "The S-motor and its applications," [44] May (1931).

52. Ackeret, "Studies on a model of a wind power plant," [45] Vol. 114, (1939).

53. Kloss, "Direct driving of synchronous generators by large wind power plants in parallel operation with a fixed-phase power system," [42] No. 31/32, (1942).

54. König, "Combined operations of coal, wind, and water" [46] p. 524 (1947).

55. Hütter, "Influence of wind frequency on 'tuning' the revolution of wind power plants," [49], No. 6 (1948) and No. 1 (1949).

56. Hütter, "Ideas regarding the exploitation of wind energy" [47], No. 1 (1950).

57. Stein, "Statistical determination and analysis of power production of wind plants" [40], No. 10 (1951).

58. Seifert, "Prospects for generating energy by wind power according to Report W/T16 of the British Electrical Industry Research Association Archives" [43], No. 23, Berlin (1950).

59. Boudineau, "A new solution for exploiting wind power" [41], No. 3 (1952).